

Analysis of a Hydroelectric Plant connected to Electrical Power System in the Physical Domain

Gilberto Gonzalez-A, Octavio Barriga

Abstract—A bond graph model of a hydroelectric plant is proposed. In order to analyze the system some structural properties of a bond graph are used. The structural controllability of the hydroelectric plant is described. Also, the steady state of the state variables applying the bond graph in a derivative causality assignment is obtained. Finally, simulation results of the system are shown.

Keywords— Bond graph, hydraulic plant, steady state.

I. INTRODUCTION

Bond graph was established by Paynter [1]. The idea was developed by Karnopp [2] and Wellstead [3] how a powerful tool of modelling. The main key of the bond graph methodology is: a model containing the energetic junction structure, *i.e.* the system architecture; different energy domains are covered and the coupling of subsystems are allowed; the cause of effect relations of each element are obtained graphically; and the state variables have a physical meaning.

Our main motivation is to apply the bond graph methodology to model a hydroelectric plant and connect to electrical power system. This methodology allows to use a variety of energy types (hydraulic, mechanical and electrical sections).

Firstly, bond graph theory is introduced by [1] modelling a basic hydroelectric plant.

In [4] and [5] describe the modelling of a hydroelectric using block diagrams and each block contains the transfer function. However, if it is necessary to change the connection of the elements or introduce new elements or reduce the model, this is difficult. Also, the analysis and control of a hydroelectric plant using block diagrams and simulation are obtained in [6] and [7]. In [8] a bond graph approach is taken to model the power system on board a supply vessel. Therefore, the contribution of this paper is to propose a bond graph model of a power system using kinetic energy water and determining the controllability and steady state analysis.

In section II describes the basic elements of the bond graph model. In section III, a bond graph model of a hydroelectric plant is proposed. The steady state of the system is presented in section IV. Also, the controllability of the system is described in section V. Section VI shows the simulations of the system and finally the conclusions are given in section 7.

Manuscript received June 25, 2008,
 Gilberto Gonzalez is with Faculty of Electrical Engineering, University of Michoacan, Mexico, (gilmichga@yahoo.com.mx)
 Octavio Barriga is with Faculty of Electrical Engineering, University of Michoacan, Mexico, (orochi_888@hotmail.com)

II. MODELLING IN BOND GRAPH

Consider the following scheme of a multiport system which includes the key vectors of Fig. 1 [3], [9].

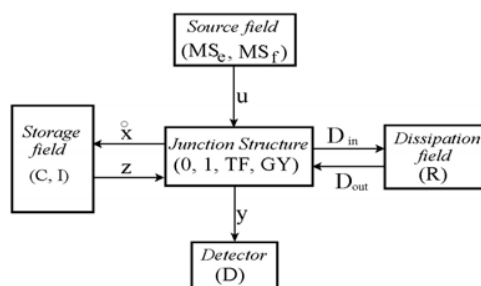


Fig. 1. Key vectors of a bond graph.

In Fig. 1, (MS_e, MS_f) , (C, I) and (R) denote the source, the energy storage and the energy dissipation fields, (D) the detector and $(0, 1, TF, GY)$ the junction structure with transformers TF , and gyrators, GY .

The state $x \in \mathbb{R}^n$ is composed of energy variables p and q associated with C and I elements in integral causality, $u \in \mathbb{R}^p$ denotes the plant input, $y \in \mathbb{R}^q$ the plant output, $z \in \mathbb{R}^n$ the co-energy vector, and $D_{in} \in \mathbb{R}^r$ and $D_{out} \in \mathbb{R}^r$ are a mixture of the power variables called effort e and flow f showing the energy exchanges between the dissipation field and the junction structure [3], [9].

The Table 1 gives the effort and flow variables for the direct formulation in some physical domains [2].

Table 1. Power variables in some energy domains.

Systems	Effort (e)	Flow (f)
Mechanical	Force (F) Torque (τ)	Velocity (v) Angular velocity (ω)
Electrical	Voltage (F)	Current (i)
Hydraulic	Pressure (P)	Volume flow rate (Q)

The relations of the storage and dissipation fields for LTI systems are,

$$z = Fx \quad (1)$$

$$D_{out} = LD_{in} \quad (2)$$

The relations of the junction structure are,

$$\begin{bmatrix} \dot{x} \\ D_{in} \\ y \end{bmatrix} = \begin{bmatrix} S_{11} & S_{12} & S_{13} \\ S_{21} & S_{22} & S_{23} \\ S_{31} & S_{32} & S_{33} \end{bmatrix} \begin{bmatrix} z \\ D_{out} \\ u \end{bmatrix} \quad (3)$$

The entries of S take values inside the set $(0, \pm 1, \pm m, \pm n)$ where m and n are transformer and gyrator modules; S_{11} and

S_{22} are square skew-symmetric matrices, and S_{12} and S_{21} are matrices each other negative transpose [9]. The state equation is,

$$\begin{aligned} \dot{x} &= A_p x + B_p u \\ y &= C_p x + D_p u \end{aligned} \quad (4)$$

where

$$A_p = (S_{11} + S_{12}MS_{21})F \quad (5)$$

$$B_p = S_{13} + S_{12}MS_{23} \quad (6)$$

$$C_p = (S_{31} + S_{32}MS_{21})F \quad (7)$$

$$D_p = S_{33} + S_{32}MS_{23} \quad (8)$$

being

$$M = (I - LS_{22})^{-1}L \quad (9)$$

Next section a bond graph model of a hydroelectric plant is proposed.

III. BOND GRAPH MODEL OF A HYDROELECTRIC PLANT

At first, the most important application for the synchronous machine was a water-turbine driven generator, making it necessary to adapt its design to the specific requirements of the hydropower plant [4].

The essential elements of the hydraulic plant are depicted in Fig. 2.

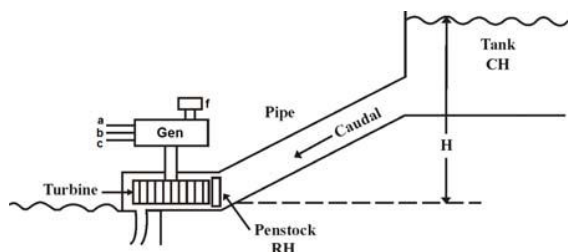


Fig. 2. Schematic of a hydroelectric plant.

The representation of the hydraulic turbine and water column in stability studies is usually based on the following assumptions [4]:

- The hydraulic resistance is negligible.
- The penstock pipe is inelastic and the water is incompressible.
- The velocity of the water varies directly with the gate opening.
- The turbine output power is proportional to the product of head and volume flow.

In according with Fig. 2 the hydroelectric plant can be divided in three sections that shows in Fig. 3.

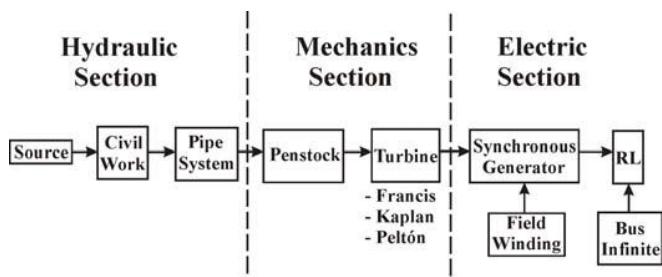


Fig. 3. Blocks diagram of a hydroelectric plant.

A. A Bond Graph Model of Hydraulic and Mechanical Sections

Hydraulic turbines are of two basic types. The impulse-type turbine (also known as Pelton wheel) is used for high heads. The high velocity jets of water impinge on spoon-shaped buckets on the runner, the change in momentum provides the torque to drive the runner, the energy supplied being entirely kinetic.

In a reaction turbine the pressure within the turbine is above atmospheric; the energy is supplied by the water in both kinetic and potential forms [4].

Precise modelling of hydraulic turbines requires inclusion of transmission line like reflections which occur in the elastic-walled pipe carrying compressible fluid. In this paper, a simple bond graph model considering the tank, the penstock and the turbine is proposed. In Fig. 4, the bond graph of the components and connection of the hydraulic and mechanical sections is shown.

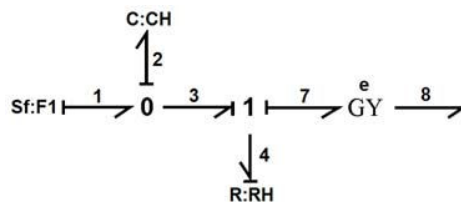


Fig. 4. Bond graph of the hydraulic and mechanical sections.

Note that the gyrator element corresponds to the converter element from hydraulic energy to mechanical energy.

B. A Bond Graph Model of a Synchronous Machine

Synchronous generators form the principal source of electric energy in power systems, many large loads are driven by synchronous motors and synchronous condensers are sometimes used as a means of providing reactive power compensation and controlling voltage. These devices operate on the same principle and are collectively referred to as synchronous machines [4], [5].

It is useful to develop mathematical models of a synchronous machine to explain their electric, magnetic and mechanical behavior. However, a graphical model of a synchronous machine is described in this section, this new model is based on bond graph model.

In this paper, the following assumptions are made for the development of a mathematical and graphical model for a synchronous machine: S_1 : the stator windings are sinusoidally distributed along the air-gap; S_2 : the stator slots cause no appreciable variation of the rotor inductances with rotor position; S_3 : magnetic hysteresis is negligible; S_4 : magnetic saturation effects are negligible.

Consider the representation of a synchronous machine of Fig. 5 [4], [5].

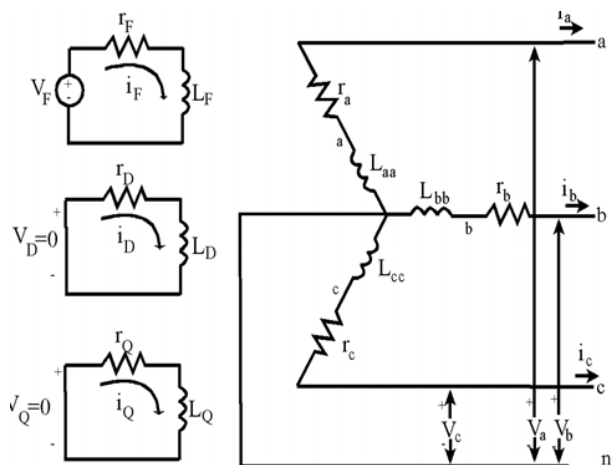


Fig. 5. Schematic diagram of a synchronous machine.

In Fig. 5, we can identify the following elements:

- a, b, c : stator phase windings. So, i_a, i_b, i_c denote the stator phase currents; v_a, v_b, v_c denote the stator phase voltages, r_a, r_b, r_c denote the stator phase resistances and L_{aa}, L_{bb}, L_{cc} denote the stator phase self inductances.
- F : field winding with i_F and v_F denote the field current and voltage, respectively; r_F denotes the field resistance and L_F denotes the field self inductance.
- D : d -axis amortisseur circuit with i_D and v_D denote the amortisseur current and voltage on the d -axis, respectively; r_D denotes the amortisseur resistance on the d -axis and L_D denotes the amortisseur self inductance on the d -axis.
- Q : q -axis amortisseur circuit with i_Q and v_Q denote the amortisseur current and voltage on the q -axis, respectively; r_Q denotes the amortisseur resistance on the q -axis and L_Q denotes the amortisseur self inductance on the q -axis.

The synchronous machine of Fig. 5, is represented by six windings are magnetically coupled. The magnetic coupling between the windings is a function of the rotor position. The instantaneous terminal voltage v of any winding is in the form,

$$v = \pm \sum r i \pm \dot{\lambda} \quad (10)$$

where λ is the flux linkage, r is the winding resistance and i is the current with positive directions of stator currents flowing out of the generator terminals.

A great simplification in the mathematical description of the synchronous machine is obtained from the Park's transformation. The effect of Park's transformation is simply to transform all stator quantities from phases a, b and c into new variables the frame of reference of which moves with the rotor. Thus by definition [5]

$$i_{odq} = P i_{abc} \quad (11)$$

where the current vectors are defined as,

$$i_{odq} = [i_0 \quad i_d \quad i_q]^T \quad (12)$$

$$i_{abc} = [i_a \quad i_b \quad i_c]^T \quad (13)$$

and the Park's transformation is

$$P = \sqrt{\frac{2}{3}} \begin{bmatrix} 1/\sqrt{2} & 1/\sqrt{2} & 1/\sqrt{2} \\ \cos \theta & \cos(\theta - 2\pi/3) & \cos(\theta + 2\pi/3) \\ \sin \theta & \sin(\theta - 2\pi/3) & \sin(\theta + 2\pi/3) \end{bmatrix} \quad (14)$$

The angle between the d axis and the rotor is given by

$$\theta = \omega_R t + \delta + \pi/2 \quad (15)$$

where ω_R is the rated angular frequency in rad/s and δ is the synchronous torque angle in electrical radians.

Similarly, to transform the voltages and flux linkages,

$$v_{odq} = P v_{abc} \quad (16)$$

$$\lambda_{odq} = P \lambda_{abc} \quad (17)$$

In according with Fig. 5, we described the bond graph model of the synchronous machine on d - q axis, in Fig. 6 that satisfies the conditions $S_1 - S_4$ of this section. This bond graph is different respect to [10] on the directions of the bonds 14, 15, 17 and 19, and we use a voltage source on the exciting winding.

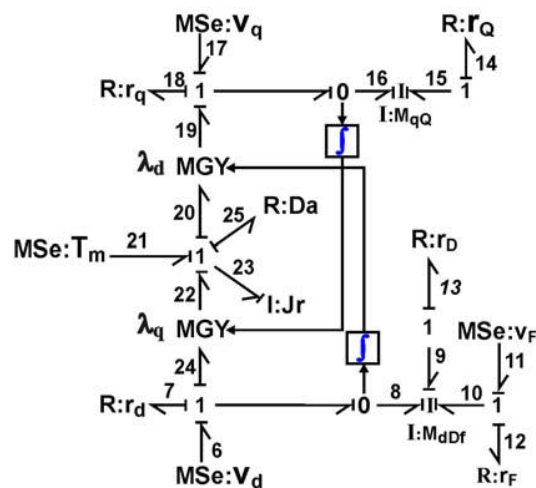


Fig. 6. Bond graph model of a synchronous machine.

In Fig. 6, T_m is the mechanical torque, J_r is the moment of inertia, D_a is the damper coefficient, $I:M_{dDF}$ and $I:M_{qQ}$ are the magnetic coupling between self and mutual inductances of the windings on d -axis and on q -axis, respectively.

C. Complete Model

The bond graph model of a hydroelectric plant is presented in Fig. 7.

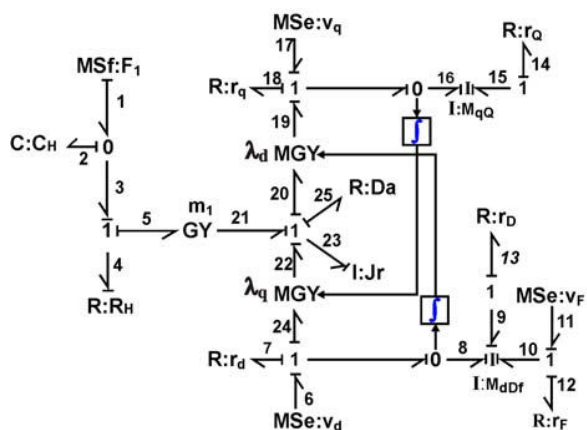


Fig. 7. Bond graph of a hydroelectric plant.

The key vectors of the bond graph are

$$x = [q_2 \ p_8 \ p_9 \ p_{10} \ p_{15} \ p_{16} \ p_{23}]^T \quad (18)$$

$$\dot{x} = [f_2 \ e_8 \ e_9 \ e_{10} \ e_{15} \ e_{16} \ e_{23}]^T$$

$$z = [e_2 \ f_8 \ f_9 \ f_{10} \ f_{15} \ f_{16} \ f_{23}]^T$$

$$D_{in} = [e_4 \ f_7 \ f_{12} \ f_{13} \ f_{14} \ f_{18} \ f_{25}]^T$$

$$D_{out} = [f_4 \ e_7 \ e_{12} \ e_{13} \ e_{14} \ e_{18} \ e_{25}]^T$$

the constitutive relations of the fields are

$$L = \text{diag} \left\{ \frac{1}{R_H}, r_d, r_f, r_D, r_Q, r_q, R_{Da} \right\} \quad (19)$$

$$F^{-1} = \text{diag} \{ C_H, M_{dDf}, M_{qQ}, J_r \} \quad (20)$$

where

$$M_{dDf} = \begin{bmatrix} L_d & m & m \\ m & L_D & m \\ m & m & L_f \end{bmatrix}; M_{qQ} = \begin{bmatrix} L_q & m_q \\ m_q & L_Q \end{bmatrix}$$

and the junction structure is,

$$S_{11} = \begin{bmatrix} 0_{6 \times 6} & g^T(\lambda) \\ -g(\lambda) & 0 \end{bmatrix} \quad (21)$$

$$S_{12} = -S_{21}^T = \begin{bmatrix} -1 & 0_{1 \times 3} & 0_{1 \times 3} \\ 0_{3 \times 1} & h & 0_{3 \times 3} \\ k & 0_{3 \times 3} & -I_3 \end{bmatrix}$$

$$S_{13} = \begin{bmatrix} I_2 & 0_{2 \times 2} & 0_{3 \times 2} \\ 0_{2 \times 2} & a_1^T & a_2^T \end{bmatrix}^T$$

where $g(\lambda) = [0 \ \lambda_q \ 0 \ 0 \ 0 \ -\lambda_d]$;

$$h = \begin{bmatrix} -1 & 0 & 0 \\ 0 & 0 & -1 \\ 0 & -1 & 0 \end{bmatrix}; k = \begin{bmatrix} 0 \\ 0 \\ r \end{bmatrix};$$

$$a_1 = \begin{bmatrix} 0 & 0 \\ 1 & 0 \end{bmatrix}; a_2 = \begin{bmatrix} 0 & 0 \\ 0 & 1 \\ 0 & 0 \end{bmatrix}$$

The nonlinear synchronous machine yields a nonlinear state equations of the complete hydroelectric plant. In this case, from (4) the nonlinear junction structure of the bond graph of the system can be defined by,

$$\dot{x}(t) = f(x(t)) + B_p u(t) \quad (22)$$

where

$$f(x(t)) = [S_{11}(\lambda) + S_{12}MS_{21}]F \quad (23)$$

By substituting (19), (20) and (21) into (23) and (6) we have,

$$f(x(t)) = \begin{bmatrix} a_{11} & a_{12} \\ a_{21} & a_{22} \end{bmatrix}$$

$$\text{where } a_{11} = \begin{bmatrix} \frac{-1}{C_H R_H} & 0 & 0 & 0 \\ 0 & \frac{-r_d}{L_d} & -mr_d & -mr_d \\ 0 & -mr_D & \frac{-r_D}{L_D} & -mr_D \\ 0 & -mr_f & -mr_f & \frac{-r_f}{L_f} \end{bmatrix};$$

$$a_{12} = \begin{bmatrix} 0 & 0 & \frac{r}{C_H J_r} \\ 0 & 0 & \frac{-\lambda_d r_{Da}}{J_r} \\ 0 & 0 & 0 \\ 0 & 0 & 0 \end{bmatrix}$$

$$a_{21} = \begin{bmatrix} 0 & 0 & 0 & 0 \\ 0 & 0 & 0 & 0 \\ \frac{r}{C_H R_H} & \frac{\lambda_q r_d}{L_d} & m\lambda_q r_d & m\lambda_q r_d \end{bmatrix};$$

$$a_{22} = \begin{bmatrix} \frac{-r_Q}{L_Q} & -mr_Q & 0 \\ -mr_q & \frac{-r_q}{L_q} & \frac{\lambda_d r_{Da}}{L_q} \\ -m\lambda_d r_d & \frac{-\lambda_d r_q}{L_q} & \frac{-1}{J_r} \left(\frac{r^2}{R_H} + r_{Da} \right) \end{bmatrix}^T$$

$$B_p = \begin{bmatrix} 1 & 0 & 0 & 0 & 0 & 0 & 0 \\ 0 & 1 & 0 & 0 & 0 & 0 & 0 \\ 0 & 0 & 0 & 1 & 0 & 0 & 0 \\ 0 & 0 & 0 & 0 & 0 & 1 & 0 \end{bmatrix}^T$$

The mathematical model to analyze the variables performance can be used. However, the next section a steady state analysis using the bond graph model is applied.

IV. STEADY STATE ANALYSIS

The response of the steady state is useful to know the value that reaches each state variable of the physical system when the dynamic period has finished. So, from (4) doing $\dot{x} = 0$, we have

$$x_{ss} = -A_p^{-1} B_p u_{ss} \quad (24)$$

where x_{ss} and u_{ss} are the steady state of the state variables and the input, respectively.

Thus, using (24) we can determine the steady state, however, we need A_p^{-1} and it is not easy to get for some high order systems. A bond graph in a derivative causality assignment to solve directly the problem of the A_p^{-1} can be applied [11].

Suppose that A_p is invertible and a derivative causality assignment is performed on the bond graph model. From (3) the junction structure is given by [11],

$$\begin{bmatrix} z \\ D_{outd} \end{bmatrix} = \begin{bmatrix} J_{11} & J_{12} & J_{13} \\ J_{21} & J_{22} & J_{23} \end{bmatrix} \begin{bmatrix} \dot{x} \\ D_{outd} \\ u \end{bmatrix} \quad (25)$$

$$D_{outd} = L_d D_{ind}$$

where the entries of J have the same properties that S . The storage elements in (25) have a derivative causality. So, D_{ind} and D_{outd} are defined of the same manner that D_{in} and D_{out} , but they depend on the causality assignment for the storage

elements and that junctions must have a correct causality assignment.

From (4) to (9) and (25) we obtain,

$$z = A_p^* \dot{x} + B_p^* u \quad (26)$$

where

$$A_p^* = J_{11} + J_{12} N J_{21} \quad (27)$$

$$B_p^* = J_{13} + J_{12} N J_{23} \quad (28)$$

being

$$N = (I - L_d J_{22})^{-1} L_d \quad (29)$$

It follows, from (1), (4) and (26) that,

$$A_p^* = F A_p^{-1} \quad (30)$$

$$B_p^* = -F A_p^{-1} B_p \quad (31)$$

From (31) and (24) we obtain the steady state,

$$x_{ss} = F^{-1} B_p^* u_{ss} \quad (32)$$

The bond graph in a derivative causality assignment of the hydroelectric plant is shown in Fig. 8.

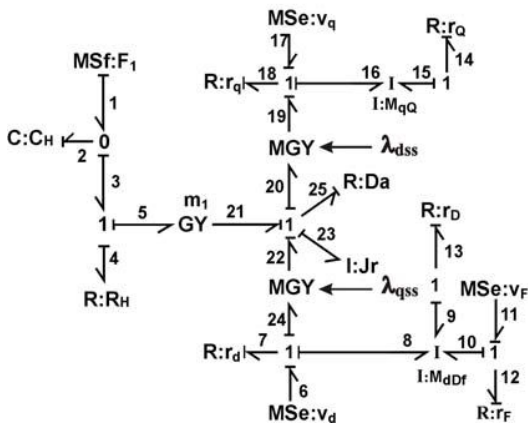


Fig. 8. Bond graph in a derivative causality assignment.

The key vectors of the bond graph in a derivative causality assignment are given in (18) and the constitutive relation of the dissipation field is $L_d = L^{-1}$ and the junction structure is

$$J_{21} = \begin{bmatrix} \alpha_{11} & 0_{4 \times 3} \\ \alpha_{21} & -I_3 \end{bmatrix}; J_{22} = \begin{bmatrix} 0_{6 \times 6} & -g^T(\lambda)_{ss} \\ g(\lambda)_{ss} & 0 \end{bmatrix}$$

$$J_{23} = \begin{bmatrix} 1 & 0 & 0 & 0 & 0 & 0 & r \\ 0 & 1 & 0 & 0 & 0 & 0 & 0 \\ 0 & 0 & 1 & 0 & 0 & 0 & 0 \\ 0 & 0 & 0 & 0 & 0 & 1 & 0 \end{bmatrix}^T; J_{11} = J_{13} = 0$$

where

$$\alpha_{11} = \begin{bmatrix} -1 & 0 & 0 & 0 \\ 0 & -1 & 0 & 0 \\ 0 & 0 & 0 & -1 \\ 0 & 0 & -1 & 0 \end{bmatrix} \quad (33)$$

$$\alpha_{21} = \begin{bmatrix} 0 & 0 & 0 & 0 \\ 0 & 0 & 0 & 0 \\ -r & 0 & 0 & 0 \end{bmatrix}$$

and $g(\lambda)_{ss}$, the steady state of $g(\lambda)$, are constants.

By substituting (19), (20), (33) into (28) we obtain

$$B_p^* = \begin{bmatrix} R_H + \frac{r^2 r_d r_q}{\Delta} & \frac{r r_q (\lambda_q)_{ss}}{\Delta} & 0 & \frac{-r r_d (\lambda_d)_{ss}}{\Delta} \\ \frac{-r r_q (\lambda_q)_{ss}}{\Delta} & \frac{(\lambda_d)_{ss}^2 + r_q r_d a}{\Delta} & 0 & \frac{(\lambda_d)_{ss} (\lambda_q)_{ss}}{\Delta} \\ 0 & 0 & \frac{1}{r_f} & 0 \\ \frac{r r_d (\lambda_d)_{ss}}{\Delta} & \frac{(\lambda_d)_{ss} (\lambda_q)_{ss}}{\Delta} & 0 & \frac{(\lambda_q)_{ss}^2 + r_d r_d a}{\Delta} \\ 0 & 0 & 0 & 0 \\ \frac{r r_d r_q}{\Delta} & \frac{r_q (\lambda_q)_{ss}}{\Delta} & 0 & \frac{-r_d (\lambda_d)_{ss}}{\Delta} \end{bmatrix} \quad (34)$$

where $\Delta = r_d (\lambda_d)_{ss}^2 + r_q (\lambda_q)_{ss}^2 + r_d r_q r_d a$.

From (20), (32) and (34) the steady state of the hydroelectric plant is determined.

By substituting the following numerical values of the parameters: $C_H = 0.578$, $R_H = 0.6$, $m_1 = 1$, $J_r = 0.0237$, $D_a = 0.25$, $r_d = r_q = 0.0011$, $r_f = 0.0742$, $r_D = 0.0131$, $r_Q = 0.054$, $L_q = 1.64$, $L_Q = 1.526$, $L_d = 1.7$, $L_D = 1.605$, $L_f = 1.65$, $M_{dDf} = 1.55$, $M_{qQ} = 1.49$, $v_f = f_1 = 1$, $v_q = 1.2245$, $v_d = 0$, $\lambda_{qss} = 0.003475$ and $\lambda_{dss} = 0.31981$ into (34) the steady state of the synchronous machine is $(e_2)_{ss} = -3.2184$, $(f_8)_{ss} = 12.062$, $(f_9)_{ss} = 0$, $(f_{10})_{ss} = 13.477$, $(f_{15})_{ss} = 0$, $(f_{16})_{ss} = 6.2342$, $(f_{23})_{ss} = -3.8184$. The complete system simulation shows the steady state of the state variables in Fig. 9 and 10.

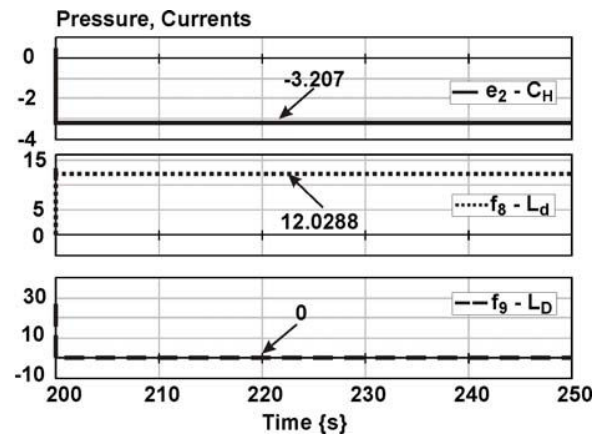


Fig. 9. Steady state of the state variables e_2 , f_8 and f_9 .

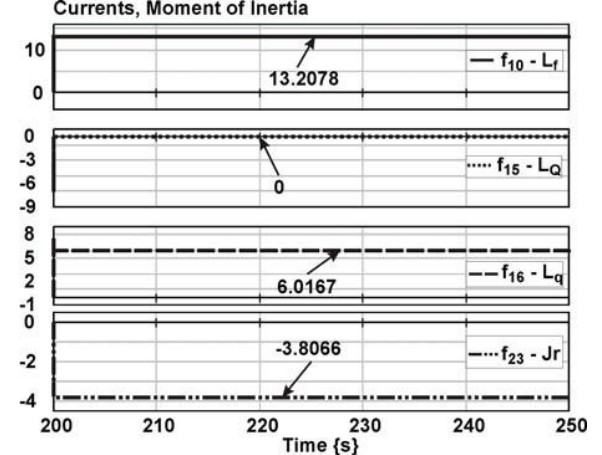


Fig. 10. Steady state of the state variables f_{10} , f_{15} , f_{16} and f_{23} .

In order to determine the steady state of the original

nonlinear system, $(\lambda_d)_{ss}$ and $(\lambda_q)_{ss}$ should be changed by λ_d and λ_q , respectively. Thus, substituting (34) into (32) with (20) we have to solve the simultaneous equations.

The following section applies the structural controllability of the hydroelectric plant in the physical domain.

V. CONTROLLABILITY ANALYSIS

The structural properties of a bond graph model that represents a physical system has received much attention such as structural controllability/observability. The great advantages of this method, such as its simplicity of implementation as well as its importance in control design and system conception are shown [9].

A linear time invariant system is completely state controllable iff:

$$\text{rank} [B_p \quad A_p B_p \quad \dots \quad A_p^{n-1} B_p] = n$$

Also, a system $[A_p B_p]$ is structurally state controllable iff [9]:

- 1) All dynamical elements in integral causality are causally connected with a source.
- 2) struct-rank $[A_p B_p] = n$.

The structural rank of $[A_p B_p]$ is equal to

- The rank of the matrix $(S_{11}S_{12}S_{13})$
- $(n - t_s)$, where n is the order of the system and t_s the number of dynamical elements remaining in integral causality when a derivative causality assignment is performed or a dualization of the maximal number of input sources is performed in order to eliminate these integral causalities.

The bond graph in an integral causality assignment of the hydroelectric plant of Fig. 7 has the following causal paths.

- For source $F_1 \rightarrow 1-2 \rightarrow C_h; F_1 \rightarrow 1-2-2-3-4-4-5-21-23 \rightarrow J_2; F_1 \rightarrow 1-2-2-3-4-5-21-23-23-22-24-8 \rightarrow M_{dDF}$ and $F_1 \rightarrow 1-2-2-3-4-4-5-21-23-23-20-19-16 \rightarrow M_{qQ}$.
- For source $V_f \rightarrow 11-10-8-24-22-23-23-21-5-4-4-3-2 \rightarrow C_H; F_1 \rightarrow 11-10-8-24-22-23 \rightarrow J_r; F_1 \rightarrow 11-10 \rightarrow M_{dDf}$ and $F_1 \rightarrow 11-10-8-24-22-23-23-20-19-16 \rightarrow M_{qQ}$.
- For source $V_d \rightarrow 6-8-8-24-22-23-23-21-5-4-4-3-2 \rightarrow C_H; V_d \rightarrow 6-8-8-24-22-23 \rightarrow J_r; V_d \rightarrow 6-8 \rightarrow M_{dDf}$ and $V_d \rightarrow 6-8-8-24-22-23-23-20-19-16 \rightarrow M_{qQ}$.
- For source $V_q \rightarrow 17-16-16-19-20-23-23-21-5-4-4-3-2 \rightarrow C_H; V_q \rightarrow 17-16-16-19-20-23 \rightarrow J_2; V_q \rightarrow 17-16-16-19-20-23-23-22-24-8$ and $V_q \rightarrow 17-16 \rightarrow M_{qQ}$.

The previous causal paths indicate that all the dynamic elements are causally connected to each source on the bond graph model in an integral causality assignment. Also, the structural rank of $[A_p B_p] = n$, because of the bond graph in a derivative causality assignment of Fig. 8 shows that all the dynamic elements have derivative causality. Thus, the bond graph of the hydroelectric system is structurally state controllable.

VI. SIMULATION OF A HYDROELECTRIC PLANT

In order to prove the controllability performance of the state variables of the proposed bond graph model, the hydroelectric

system simulation using the software 20-Sim with the numerical parameters of the previous section is presented. Fig. 11 presents a block diagram in 20-Sim.

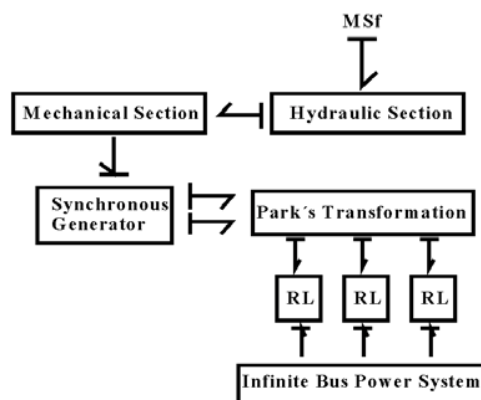


Fig. 11. Block diagram in 20-Sim.

Fig. 12 shows the variable performance e_2 when the input changes from $F_1 = 1$ to $F_1 = 3$ and $V_f = 1$ to 2 and 4.

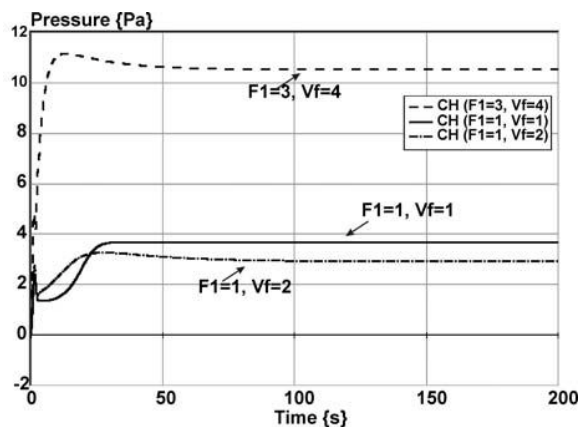


Fig. 12. Variable performance e_2 .

Also, the state variables behavior of the amortisseur circuits f_9 and f_{15} are shown in Fig. 13, where the steady state of both amortisseurs are zero.

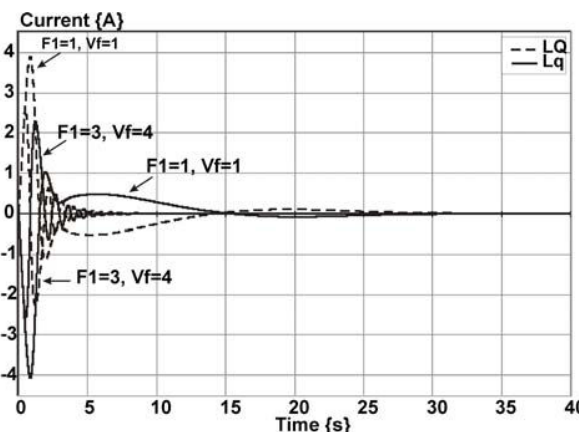


Fig. 13. State variables behavior p_9 and p_{15} .

In addition, the dynamic and steady state periods of state variables f_8 , f_{10} and f_{16} are illustrated in Fig. 14. Note that these are the most important variables to the power system. So, these variables are controllable by the sources F_1 and V_f .

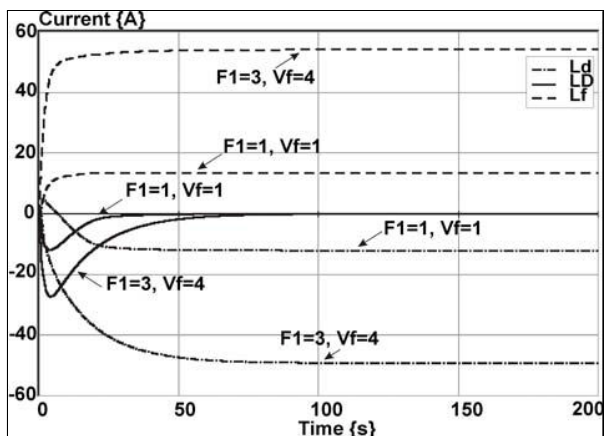


Fig. 14. State variables performance f_8 , f_{10} and f_{16} .

The variable response p_{23} is shown in Fig. 15 indicating that this variable can be controllable by the two sources.

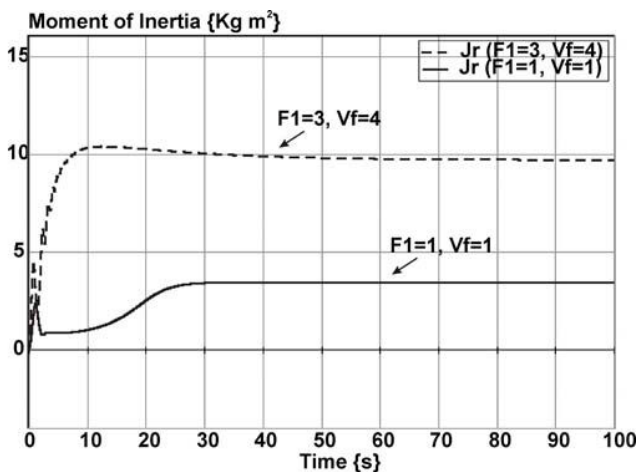


Fig. 15. Variables response f_{23} .

Finally, Fig. 16 shows the three phase currents on the loads RL that connects the hydroelectric plant with the infinite bus power system.

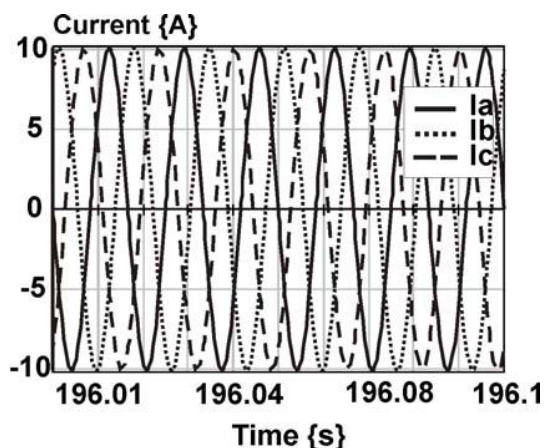


Fig. 16. Three phase currents of the system.

Therefore, the bond graph model of the hydroelectric plant allows to know the dynamic and steady state performance, controllability, reconfiguration and simplified models in a simple and direct manner.

VII. CONCLUSIONS

A bond graph model of a hydroelectric plant is presented. Important characteristics of the system as controllability and steady state in the physical domain can be obtained. In order to verify the state variables performance, simulation results are given.

REFERENCES

- [1] H. M. Paynter, *Analysis and design of engineering systems*, MIT press, Cambridge, Mass, 1961.
- [2] Dean C. Karnopp, Donald L. Margolis and Ronald C. Rosenberg, *System Dynamics Modeling and Simulation of Mechatronic Systems*, Wiley, John & Sons, 2000.
- [3] P. E. Wellstead, *Physical System Modelling*, Academiv Press, London, 1979.
- [4] John R. Kundur, *Power System Stability and Control*, Mc-Graw-Hill, 1994
- [5] P. M. Anderson, *Power System Control and Stability*, The IOWA state University Press, 1977.
- [6] F. Irie, M. Takeo, S. Sato, O. Katahira, F. Fukui, H. Okada, T. Ezaki, K. Ogawa, H. Koba, M. Takamatsu and T. Shimojo, *A Field Experiment on Power line Stabilization by a SMES System*, IEEE Transactions on Magnetics, Vol. 28, No. 1 January 1992.
- [7] D. B. Arnavotic and D. M. Skataric, *Suboptimal Design of Hydroturbine Governors*, IEEE Transactions on Energy Conversion, Vol. 6, No. 3, September 1991.
- [8] Toma Arne Pedersen and Elif Pedersen, *Bond Graph Model of a Supply Vessel Operating in the North Sea*, Proceedings of the 2007 International Conference on Bond Graph Modeling
- [9] C. Sueur and G. Dauphin-Tanguy, *Bond graph approach for structural analysis of MIMO linear systems*, Journal of the Franklin Institute, Vol. 328, No. 1, pp. 55-70, 1991.
- [10] Dietrich Sahn, *A two-Axis, Bond Graph Model of the Dynamics of Synchronous Electrical Machine*, Journal of the Franklin Institute, Vol. 308, No. 3, pp. 205-218, 1979.
- [11] Gilberto Gonzalez-A and R. Galindo, *Steady State Values for a Physical System with a Bond Graph Approach*, Proceedings of 9th IEEE International Conference Methods and Models in Automation and Robotics, pp. 1317-1322, 2003.